

### Variable cell-shape molecular dynamics

José Luís Martins

Departamento de Física, Instituto Superior Técnico,  
Avenida Rovisco Pais 1, 1096 Lisboa, Portugal

and

Instituto de Engenharia de Sistemas e Computadores,  
Rua Alves Redol 9, Apartado 13069, 1000 Lisboa, Portugal

#### Abstract

One problem frequently encountered in the simulation of real materials, like amorphous solids, liquids, complex surfaces or defects, is that the positions of the constituent atoms are not well known from experiment, and must be determined from the calculations. This can be done with Monte Carlo or molecular dynamics simulations based on the calculation of the total energy of the system. If the volume or cell shape of the material is not known, then variations in cell shape have to be included in the simulation. Here we review briefly variable cell-shape molecular dynamics methods, present a new approach, and give a few examples of variable cell-shape molecular dynamics and structural optimization for  $\text{MgSiO}_3$ , Si and ternary Ca nitrides using forces calculated from first principles.

#### 7.1 INTRODUCTION

With the development of new simulation methods and the increase in available computational power, molecular dynamics has become an important tool in the simulation of matter in the condensed state [1, 2]. In its simplest applications, molecular dynamics is used to integrate Newton's equations of motion for the nuclei subject to empirical forces. For example, one would choose a Lennard-Jones potential to simulate liquid argon, or a Born-Mayer potential to simulate NaCl. Starting with the Car-Parrinello method, [3] it has been possible to use in molecular dynamics simulations forces that are determined from first principles quantum-mechanical calculations of the electronic structure.

In the simplest molecular dynamics schemes, the shape of the simulation cell and number of particles are held constant, and the integration of Newton's equation of motion with forces derived from a potential conserves the energy (within the precision of the integration scheme), and one expects to be simulating a micro-canonical ensemble. However, in laboratory conditions,

one often controls the intensive variables temperature  $T$  and pressure  $p$ , instead of the extensive variables  $E$  and  $V$ . Therefore more subtle molecular dynamics schemes were developed to simulate systems at constant temperature or pressure [1, 2, 4, 5, 6, 7, 8]. In the case of constant pressure simulations, the size and shape of the simulation cell must be allowed to change. In order to do so, an “extended system” is constructed which includes degrees of freedom for the cell. A microscopic simulation of the structural, mechanical, and dynamical response of material systems to external stress of interest in tribology, material fatigue and wear, crack propagation, stress induced phase and structural transformations, lubrication and hydrodynamical phenomena, is more conveniently done with varying cell shapes. In this highlight we review briefly variable cell-shape molecular dynamics methods, present a new approach, and give a few examples of structural optimization from first principles.

## 7.2 VARIABLE CELL-SHAPE MOLECULAR DYNAMICS

Andersen [6] proposed to use the volume  $V$  of a cubic simulation cell as a dynamical variable in an extended hamiltonian, thus allowing for volume fluctuations (but not shape fluctuations) driven by the dynamical imbalance between the imposed external pressure,  $p_{\text{ext}}$ , and the actual instantaneous internal pressure,  $p_{\text{int}}$  (given by the virial theorem). As the simulation cell is periodically repeated, the dynamics associated with the cell is not physical, but is a computational trick to allow a relaxation of the cell. In the extended lagrangian for the dynamics, Andersen included a fictitious kinetic energy term associated with the rate of change of volume,

$$K_{\text{cell}}^{\text{A}} = \frac{W^{\text{A}}}{2} \dot{V}^2, \quad (1)$$

where  $W^{\text{A}}$  is a fictitious “mass” associated with the cell. He also added the term  $U_{\text{cell}} = p_{\text{ext}}V$ , which is the potential from which the constant external pressure acting on the cell is derived. During the simulations, the volume  $V$  fluctuates about an average value such that, in the limit of long simulation times, the time average of the calculated internal pressure is equal to the chosen external pressure,  $\bar{p}_{\text{int}} = p_{\text{ext}}$ . The equations of motion can be derived from the Lagrangian,

$$\mathcal{L}_A = K_{\text{cell}}^{\text{A}} + \frac{1}{2} \sum_k m(k) \dot{r}^2(k) - U_{\text{model}} - p_{\text{ext}}V \quad (2)$$

where  $r(k)$  is the position of particle  $k$ , and  $U_{\text{model}}$  is our interatomic potential (Lennard-Jones, Kohn-Sham total energy etc...).

Andersen’s method is best suited to study equilibrium properties of fluids, for which the shape of the cell is irrelevant. To study shear flow (viscosity) in fluids or to study solids it is not enough to change volume with constant shape. For example, a given cell shape may be compatible with the periodicity of one crystal structure and be incompatible with another solid phase, and so the fixed cell shape may artificially prevent the appearance of thermodynamically more stable phases. In order to study structural phase transitions, Parrinello and Rahman [7, 8] extended Andersen’s method to allow for changes in both the volume and the shape of the cell. They used as dynamical variables the cartesian components

$$h_{ij} = \vec{e}_i \cdot \vec{a}_j$$

of the three vectors  $\vec{a}_j$  defining the periodicity of the simulation cell. Here  $\vec{e}_i$  are the three orthonormal vectors that define a cartesian coordinate system. To generate the dynamics, a fictitious kinetic energy of the cell

$$K_{\text{cell}}^{\text{PR}} = \frac{W^{\text{PR}}}{2} \sum_{i=1}^3 \sum_{j=1}^3 (\dot{h}_{ij})^2, \quad (3)$$

is defined, where  $W^{\text{PR}}$  is again a fictitious mass. Several authors have pointed out some shortcomings of the original method of Parrinello and Rahman: it is not invariant under modular transformations (defined below), the consistency between the condition of mechanical equilibrium and the virial theorem is only verified in the large  $N$  limit, and it has spurious cell rotations [9, 10, 11, 12].

For a given periodic system, there are infinite equivalent choices of the basic simulation cell. If  $\vec{a}_i$  are three vectors commensurate with the periodic system, then the transformation  $\vec{a}'_j = \sum_k M_{kj} \vec{a}_k$ , with  $M$  an integer matrix with  $|\det M| = 1$ , gives another set of vectors describing the periodicity. It is desirable that the dynamics should not depend on the particular choice that is made, i.e., the equations of motion should be formally invariant with respect to the interchange between equivalent cells (modular transformations) [9, 10]. This characteristic improves the physical content of the simulation, by eliminating symmetry breaking effects associated with the fictitious part of the dynamics [10]. Of course, in the thermodynamic limit ( $N \rightarrow \infty$ ) these effects vanish, but they may be important in computer simulations, which may use only a small number of particles. That is often the case in first-principles molecular dynamics [3].

The orientation in space of the simulation cell is irrelevant for the structural and thermodynamical description of the system (principle of material-frame indifference [12]). However, it is included in the dynamics if one uses the components of the cell edges as dynamical variables, and spurious cell rotations have been obtained in actual simulations with the Parrinello-Rahman method, namely in the simulation of molecules, whose internal degrees of freedom sometimes cause the internal stress to be asymmetrical [13]. Methods to eliminate them have been proposed, such as constraining the matrix of the lattice vectors to be symmetrical [13] or upper triangular [14] (geometrical constraints), or by symmetrization of the infinitesimal strain at each time step (dynamical constraint) [12].

A Lagrangian that is invariant with respect to modular transformations was proposed by Cleveland. [9] He used

$$K_{\text{cell}}^{\text{Cl}} = \frac{W^{\text{Cl}}}{2} \text{Tr}(\dot{h} A^T A \dot{h}^T), \quad (4)$$

as the cell kinetic energy, where the matrix  $A$  is defined by  $A = \{\vec{a}_2 \times \vec{a}_3, \vec{a}_3 \times \vec{a}_1, \vec{a}_1 \times \vec{a}_2\}$ , and is related to the reciprocal lattice vectors. The interpretation of the definition in equation 4 is not trivial. Wentzcovitch rederived similar expressions, [10] but she also suggested the use of other dynamical variables in the simulation, namely the *symmetric* stress tensor  $\epsilon$ , and showed that from the cell kinetic energy

$$K_{\text{cell}}^{\text{W}} = \frac{W^{\text{W}}}{2} \text{Tr}(\dot{\epsilon} \dot{\epsilon}^T), \quad (5)$$

one obtained a Lagrangian that is invariant with respect to modular transformations. The stress tensor is defined with respect to a reference cell shape,  $h = (1 + \epsilon)h_0$ . The initial cell shape is arbitrary, and the dependence of the dynamics on that choice can be removed by using what in

material science is called the true stress,  $h = \exp(\epsilon)h_0$  instead of the engineering stress defined previously.

The symmetrical metric tensor,

$$g_{ij} \equiv \vec{a}_i \cdot \vec{a}_j = g_{ji},$$

defines all the geometric properties of the simulation cell. Using it as a variable for the dynamics, allows us to cast the problem in a metric language and simplifies the search for good cell kinetic energies because only scalar expressions are acceptable. [15] A simple non-negative scalar that is quadratic in the time derivatives of all the components of  $g$  is

$$K_{\text{cell}}^g(g_{ij}, \dot{g}_{ij}) = \frac{W^g}{2} (\det g_{ij}) \dot{g}_{ji} (g^{ik} \dot{g}_{kl} g^{lj}), \quad (6)$$

where  $W^g$  is a fictitious cell “mass” with the dimensions of mass times length<sup>-4</sup>.

The fictitious Lagrangian for the extended system in the presence of an applied external pressure in this case is

$$\mathcal{L}_2(s^i(k), \dot{s}^i(k), g_{ij}, \dot{g}_{ij}) = \frac{1}{2} \sum_k m(k) \dot{s}^i(k) g_{ij} \dot{s}^j(k) - U(s^i(k), g_{ij}) + \frac{W^g}{2} (\det g_{ij}) \dot{g}_{ji} g^{ik} \dot{g}_{kl} g^{lj} - p_{\text{ext}} \sqrt{\det g_{ij}}, \quad (7)$$

where the  $s^j(k)$  are the atomic lattice coordinates defined by  $\vec{r}(k) = s^j(k) \vec{a}_j$ .

### 7.3 ANISOTROPIC EXTERNAL STRESS

A constant applied anisotropic stress is in general non-conservative, and thus there is no conserved extended hamiltonian in a constant anisotropic stress simulation [9, 16]. Of course some experimental situations are essentially non-conservative, and therefore best simulated by an appropriate non-conservative dynamics [9, 16].

Molecular dynamics simulations with an applied anisotropic stress were first proposed by Parinello and Rahman [8]. Ray and Rahman [17] later showed that the original formulation was valid only in the limit of small deformations, and they proposed an extension valid for finite deformations, in which it is the thermodynamic tension [17, 18]

$$\tau = \frac{V}{V_0} h_0 h^{-1} \sigma_{\text{ext}}^{\text{cart}} (h^T)^{-1} h_0^T, \quad (8)$$

where  $h_0$  and  $V_0$  are the reference lattice and its volume, and  $\sigma_{\text{ext}}^{\text{cart}}$  is the external stress in cartesian coordinates. The physical interpretation of the thermodynamic tension is not trivial.

The thermodynamic variable conjugate to the metric is  $\sigma_{\text{ext}}^{ij}$ , the external stress in contravariant lattice coordinates. [15] Keeping it constant when the cell deforms leads to a conservative external stress, if one uses the potential

$$U_{\text{cell}}(g) = \frac{1}{2} \sigma_{\text{ext}}^{ji} g_{ij}, \quad (9)$$

The metric notation is quite compact when compared with the definition of  $\tau$  in Eq. 8.

## 7.4 STRUCTURAL OPTIMIZATION

A problem encountered in the simulation of materials is the determination of the equilibrium structure of a crystal at a given pressure (or anisotropic stress) predicted by a given model  $U(s^i(k), g_{ij})$  of its total energy. This can, in principle, be achieved by the minimization (under the appropriate constraint) of  $U$ , which is quite difficult because it is a multivalleyed function of many variables. A practical strategy is to use a simulated annealing to bring the configuration to a deep valley, followed by a search of a minimum in that valley. The annealing step can be carried out by the variable cell shape molecular dynamics described previously coupled to a thermostat, brownian dynamics forces, or a periodic rescaling of the velocities. The local minimization can be done efficiently if one has the gradient of the function to be minimized.

If we want to obtain the crystal structure at zero temperature and for an applied pressure of  $p_{\text{ext}}$ , we must minimize its enthalpy,

$$H(s^i(k), g_{ij}) = U(s^i(k), g_{ij}) + p_{\text{ext}} \sqrt{\det g_{ij}}.$$

The gradient of the enthalpy with respect to atomic positions is

$$\frac{\partial H}{\partial s^i(k)} = \frac{\partial U}{\partial s^i(k)} = -F_i(k),$$

which is minus the covariant components of the force on that atom. Notice that in molecular dynamics derived from the Lagrangian of Eq. 7, it is the contravariant components,  $F^i(k) = g^{ij} F_j(k)$  that appear in the equation of motion. The gradient of the enthalpy with respect to the metric is

$$\frac{\partial H}{\partial g_{ij}} = \frac{\partial U}{\partial g_{ij}} + \frac{1}{2} p_{\text{ext}} g^{ij} \sqrt{\det g_{ij}}.$$

These gradients can be fed into any gradient based minimization algorithm to optimize the crystal structure for a chosen external pressure  $p_{\text{ext}}$ .

## 7.5 APPLICATIONS

Table I shows a comparison of calculated and experimental structural constants for  $\text{MgSiO}_3$ , a mineral with a distorted perovskite of geological importance. The calculations were done using the strain tensor as the dynamical variable, and a damped dynamics minimization scheme. [19] The structure is orthorhombic with lattice constants, a, b, and c, the other lines in the table give the atomic coordinates. The last column gives what the values would be for an undistorted perovskite structure. It is clear from the table that one can optimize quite complicated structures, and that LDA is successful in the prediction of ground state properties of complex silicates.

Figure 1 shows the results of a first principles simulation of Si under pressure using the metric as variable. A similar simulation using the Parrinello-Rahman Lagrangian was done previously. [20]

It is well-known that silicon undergoes several phase transformations with increasing pressure, and its pressure-volume phase diagram has been extensively studied [21]. Starting from a diamond lattice, the structure changes at  $\sim 11$  GPa into  $\beta$ -Sn, and between 13 and 16 GPa transforms into simple hexagonal. Other densely packed phases appear at around 38 GPa. In the first

	Calc.(Pbnm)	Exp.(Pbnm)	Undistorted
a	4.711	4.777	4.909
b	4.880	4.927	4.909
c	6.851	6.898	6.942
$Mg_x$	0.5174	0.5131	0.500
$Mg_y$	0.5614	0.5563	0.500
$O_x^1$	0.1128	0.1031	0.000
$O_y^1$	0.4608	0.4654	0.500
$O_x^2$	0.1928	0.1953	0.250
$O_y^2$	0.1995	0.2010	0.250
$O_z^2$	0.5582	0.5510	0.500

Table 1: Experimental and theoretical parameters of the zero pressure  $Pbnm$  phase of  $MgSiO_3$ . This phase (four  $MgSiO_3$  units) has Si atoms located at  $(1/2, 0, 0)$ ,  $(1/2, 0, 1/2)$ ,  $(0, 1/2, 0)$ , and  $(0, 1/2, 1/2)$ , Mg's at  $\pm(Mg_x, Mg_y, 1/4)$ ,  $\pm(1/2 - Mg_x, Mg_y + 1/2, 1/4)$ , and two sets of inequivalent O's at  $\pm(O_x^1, O_y^1, 1/4)$ ,  $\pm(1/2 - O_x^1, O_y^1 + 1/2, 1/4)$  and  $\pm(O_x^2, O_y^2, O_z^2)$ ,  $\pm(1/2 - O_x^2, O_y^2 + 1/2, 1/2 - O_z^2)$ ,  $\pm(O_x^2, O_y^2, O_z^2 + 1/2)$ ,  $\pm(1/2 + O_x^2, 1/2 - O_y^2, O_z^2)$ .

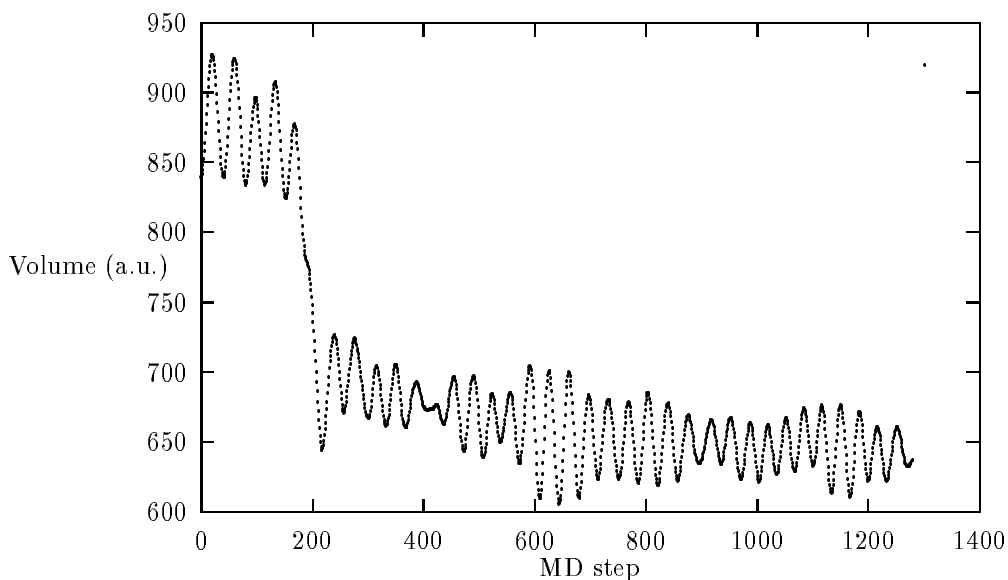


Figure 1: The volume (in atomic units) of an eight-atom Si cell is shown as a function of the molecular dynamics step in a first-principles simulation with an applied pressure of 25 GPa. The volume starts by oscillating around the volume of the initial diamond phase, but after 200 steps shows a rapid decrease to values near the equilibrium value at 25 GPa.

$\sim 0.7$  ps (200 steps) of the simulation, we observed (Fig. 1) that the volume of the simulation cell was fluctuating around a value that corresponds to the volume of the metastable diamond structure of Si at 25 GPa ( $V \sim 885$  a.u. for the 8 atoms of the conventional cubic unit cell). There was then a rapid drop in the volume, accompanied by a rapid rise in the ionic temperature to around 3500K (well above the melting point). The simulation was interrupted after 1000 steps, well before equilibrium with the thermal bath was reached. After the transition, the volume of the cell oscillated around 650 a.u., slightly below the volume of the stable simple hexagonal

	Experimental	Theoretical	Experimental	Theoretical
compound	AsN <sub>3</sub> Ca <sub>3</sub>	AsN <sub>3</sub> Ca <sub>3</sub>	PNCa <sub>3</sub>	PNCa <sub>3</sub>
$a$ (Å)	6.716	6.720	6.709	6.707
$b$ (Å)	6.711	6.715	6.658	6.659
$c$ (Å)	9.520	9.526	9.452	9.451
$\Delta_1$	0.0329	0.0400	—	0.0464
$\Delta_2$	0.0321	0.0400	—	0.0459
$\delta$	0.0209	0.0265	—	0.0396
$\gamma_1$	0.0399	0.0510	—	0.0747
$\gamma_2$	0.0048	0.0100	—	0.0220
$\lambda_1$	0.0000	0.0032	—	0.0084
$\lambda_2$	0.0170	0.0263	—	0.0449

Table 2: Experimental and numerical results for the lattice and distortion parameters of AsN<sub>3</sub>Ca<sub>3</sub> and PNCa<sub>3</sub>.

structure at that pressure, but above the density of the close-packed structures. Remembering that at atmospheric pressure Si contracts upon melting, and considering the high temperatures of the simulation, our results indicate that at high pressures, the liquid phase may still be denser than the solid phase.

Table II shows the results of an optimization of the structure of ternary calcium nitrides using the metric as variable, [22] compared to the experimental results. [23] The material is an anti-perovskite, and again the distortions from the ideal crystal (small parameters in the table) is correctly predicted by the calculations. This last results are from a Lisbon-Antwerp collaboration that received psik support.

## 7.6 CONCLUSIONS

Variational cell-shape molecular dynamics can be used in structural optimization, or the simulation of phase transitions. It is only recently that it started being applied to real materials with forces and stresses derived from first principles total energy calculations. As the dynamics of the cell is fictitious, the choice of the kinetic energy associated with the cell motion is not unique. In fact even a choice of the dynamical variables associated with the cell motion has to be made. The original choice for the cell variables were the cartesian components of the cell vectors, but choosing the strain tensor or the metric tensor has some advantages. We expect that first-principles variational cell-shape molecular dynamics will become a very useful tool in the study of equilibrium structures in crystals at a fixed pressure.

## References

- [1] M. P. Allen and D. J. Tildesley, in *Computer Simulation of Liquids* (Oxford University Press, Oxford, 1987).

- [2] D. Frenkel and B. Smit, in *Understanding Molecular Simulation* (Academic Press, 1996).
- [3] R. Car and M. Parrinello, Phys. Rev. Lett. **55**, 2471 (1985).
- [4] S. Nosé, Mol. Phys. **52**, 255 (1984).
- [5] R. Biswas and D. R. Hamann, Phys. Rev. B **34**, 895 (1986).
- [6] H. C. Andersen, J. Chem. Phys. **72**, 2384 (1980).
- [7] M. Parrinello and A. Rahman, Phys. Rev. Lett. **45**, 1196 (1980).
- [8] M. Parrinello and A. Rahman, J. Appl. Phys. **52**, 7182 (1981).
- [9] C. L. Cleveland, J. Chem. Phys. **89**, 4987 (1988).
- [10] R. M. Wentzcovitch, Phys. Rev. B **44**, 2358 (1991).
- [11] J. R. Ray, J. Chem. Phys. **79**, 5128 (1983).
- [12] J. V. Lill and J. Q. Broughton, Phys. Rev. B **49**, 11619 (1994) and references cited therein.
- [13] S. Nosé and M. L. Klein, Mol. Phys. **50**, 1055 (1983).
- [14] G. Ciccotti and J. P. Ryckaert, Comput. Phys. Rep. **4**, 345 (1986).
- [15] I. Souza and J. L. Martins, Phys. Rev. B **55** (1997). Scheduled for April 1st.
- [16] M. W. Ribarsky and Uzi Landman, Phys. Rev. B **38**, 9522 (1988).
- [17] J. R. Ray and A. Rahman, J. Chem. Phys. **80**, 4423 (1984).
- [18] R. N. Thurston, in *Physical Acoustics: Principles and Methods*, edited by Warren P. Mason (Academic, New York, 1964), pp. 1-110.
- [19] R. M. Wentzcovitch, J. L. Martins, and G. D. Price, Phys. Rev. Lett. **70**, 3947 (1993).
- [20] P. Focher, G. L. Chiarotti, M. Bernasconi, E. Tosatti and M. Parrinello, Europhys. Lett., **26**, 345 (1994).
- [21] J. Zhu Hu, L. D. Merkle, C. S. Menoni and I. L. Spain, Phys. Rev B **34**, 4679 (1986).
- [22] P.R. Vansant, P.E. Van Camp, V.E. Van Doren, and J.L. Martins, to be published.
- [23] M.Y. Chern, D.A. Vennos and F.J. Disalvo; J. Sol. Stat. Chem. **96**, 415-425 (1992). M.Y. Chern, F.J. Disalvo, J.B. Parise and J.A. Goldstone; J. Sol. Stat. Chem. **96**, 426-435 (1992).